

Optical Quasipatterns

M. LE BERRE, D. LEDUC, E. RESSAYRE AND A. TALLET

*Laboratoire de PhotoPhysique Moléculaire du CNRS
Bât.210, Université Paris-sud, 91405 Orsay cedex, France*

Abstract

Quasiperiodic patterns originate from multicriticality. The mechanisms for the formation of these structures are discussed for optical devices that display different types of nonlinearities. Numerical patterns illustrate the multiple scale analysis predictions.

I-Introduction

This article is written to commemorate the untimely passing away of Professor Marko Jaric, whose work on quasicrystals produced a lasting impact on the field.

The formation of optical patterns has been mainly studied in **single longitudinal mode** devices with either active or passive media. In such cases, the systems may develop a stationary transverse oscillation, leading to periodic patterns like rolls, squares and hexagons or to a travelling transverse wave. Spatial solitons, vortices, localized structures may also occur and are presently extensively studied¹.

Actually, most devices operate on several longitudinal modes and, consequently display a multiconical emission of light². The inner ring corresponds to the largest wavelength that is the only one to be considered in the mean-field models³. (For a discussion, see Ref. [4]). Therefore, the experimental set-up for the observation of structures predicted within the framework of the single-mode model requires some low-K filtering procedure^{5,6}. But, if the outer rings of the multiconical emission of light are not suppressed, smaller transverse wavelengths may participate in the growth of instabilities⁷⁻¹⁵: It often appears that the new patterns are no longer invariant under space translation¹⁶, leading to two-dimensional quasicrystals.

Quasicrystals¹⁷ have been discovered in three-dimensional lattices by Shechtman *et al* in 1984 and then extensively studied¹⁸, even recently in optics where cold atoms localize in quasiperiodical lattices built with laser beams¹⁹.

Two-dimensional quasi-structures have been also observed: The generation of a twelvefold orientational order pattern was first reported by Edwards and Fauve²⁰ in a Faraday instability experiment, where the capillary waves were excited by a two-frequency force. Eightfold and tenfold orientational order patterns were observed in a Faraday instability in case of a single frequency parametric excitation^{21,22}. And quite recently in optics, the group of W. Lange has observed both the eightfold and the twelvefold quasipatterns on the laser light profile in a single-feedback experiment with a sodium vapor¹⁵.

The formation of these 2N-fold orientational order structures as a result of the coexistence of N Fourier active modes was first analyzed by H. Müller²³. More precisely, two types of nonlinear selection mechanisms were assumed, either monocritical or bicritical, depending on the presence of one or two sets of active modes. A 2N-fold orientational order monocritical pattern was predicted to occur when the N modes are coupled by a cubic interaction with an appropriate Landau coefficient. Differently, the mechanism for the formation of a bicritical pattern lies on a resonance condition that requires a magic ratio between the two critical wavenumbers in order that the tryadic interaction between the modes works. The formation of the twelvefold orientational order structure^{15,20} belongs to this case²³.

These mechanisms have been discussed by us in optical systems^{4,10,11}. An eightfold orientational order monocritical pattern was predicted to occur in case of a polarization

instability in a rubidium vapor⁸ and a bicritical twelvefold orientational order pattern was found to occur when the input beam is circularly polarized^{15,24}. Bicritical twelvefold orientational order patterns were also reported with a liquid crystal light valve^{12,13} and a periodic bisquare was displayed in the ring cavity with two-level atoms¹¹. With the degenerate optical parametric oscillator (DOPO), both monocritical and bicritical quasipatterns were shown to occur⁴.

The $2N$ -fold orientational order patterns display quasiperiodicity because they are built with the help of two wavenumbers: The first one is the critical wavenumber, i.e. the radius of the circle on which the maxima are distributed in the far-field, and the second one is the chord between two adjacent maxima, associated to the vertex angle $\frac{\pi}{N}$. Generally the ratio between these two wavenumbers is irrational, leading to a quasiperiodic behaviour. The particular case, for which the chord is equal to the radius, displays a wavenumber locking leading to the well-known hexagonal lattice. (The cases of a single-mode or a two-mode structure are not in discussion because they are automatically periodic in a two-dimensional space).

There are also structures such that the $2N$ modes are not regularly distributed on the circle^{10b}. In that case there are generally at least three wavenumbers for the characterization of the structure. If no locking mechanism occurs, then the structure will generally present chaotic properties. (See §IIb).

In optics, multicriticality is the result of the propagation of the light beam in the free space in between its exit from the nonlinear medium to its feedback into the medium, with the help of one (single-feedback mirror device) or several mirrors (ring cavity device). Indeed, let us assume that the amplitude of the signal is proportional to a Fourier mode at the exit of the medium, $\varepsilon_s \propto e^{i\vec{K}_0 \cdot \vec{r}}$. After it propagates in the free-space on the length L , the signal diffracts like $e^{iL\nabla^2/2k} e^{i\vec{K}_0 \cdot \vec{r}}$, i.e. $e^{-iLK_0^2/2k} e^{i\vec{K}_0 \cdot \vec{r}}$: If $K_0 = |\vec{K}_0| \sqrt{L/2k}$ is the fundamental critical wavenumber, then there are an infinite number of solutions,

$$K_n = \sqrt{K_0^2 + n\pi}, \quad (1)$$

which are alternatively associated with a modulational instability for even n and with a wave instability¹⁴ (modulational + Hopf bifurcation, with a period equal to $\frac{2L}{c}$) for odd n .

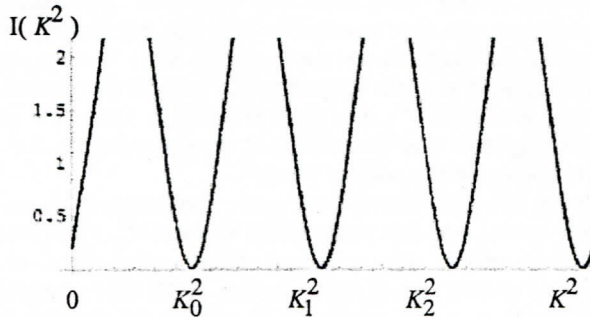


Fig.1

Therefore, in any optical device where the diffraction effects appear mainly in the free-space, the marginal stability curve presents an infinite set of minima located at K_n , with a degenerate

threshold intensity in absence of diffusion process (see Fig. 1). The multicritical patterns originate in this multiconical emission process.

In the next sections, two different kinds of nonlinear systems are investigated: In Section II, the **monocritical** mechanism is discussed for the single-feedback mirror device with a rubidium vapor, when the polarisation of the signal is orthogonal to the linear polarization of the pump and for the DOPO displaying a $\chi^{(2)}$ nonlinearity. While the original equations describing these two systems are quite different, the multiple scale analysis gives rise to amplitude equations with a cubic nonlinearity between the Fourier modes. The study of these amplitude equations leads to the prediction of different quasiperiodic structures. Section III treats the **bicritical** case. The mechanism of the formation of bisquares in the passive ring cavity device with two-level atoms is analyzed with the help of a bicritical multiple scale analysis. The twelvefold quasipattern that occurs in the single-feedback device, when the rubidium gas cell is excited by a circularly polarized pump, is also analyzed.

II-Monocritical bifurcations

Let us assume $Q(\vec{r}, t)$ to be the control parameter for the considered system, and expand it as a superposition of N Fourier modes,

$$Q(\vec{r}, t) = \sum_{p=1}^N A_p(t) e^{i\vec{K}_p \cdot \vec{r}} + c.c. \quad , \quad |\vec{K}_p| = K_c \quad p = 1, N \quad (2)$$

The amplitude equations for the polarization instability of a rubidium gas¹⁰ and the DOPO⁴ are the standard equations for a supercritical bifurcation with a cubic nonlinearity between the modes,

$$\partial_t A_\ell = \mu A_\ell - A_\ell \left[|A_\ell|^2 + \sum_{p \neq \ell}^N \beta_{\ell p} |A_p|^2 \right] \quad (3)$$

where the coefficient μ is proportional to the intensity shift from the threshold. The Landau coefficient $\beta_{\ell p}$ depends on the vertex angle between the two modes \vec{K}_ℓ and \vec{K}_p , $\theta_{\ell p} = (\vec{K}_\ell, \vec{K}_p)$, with $0 < \theta < \pi$. It has to be small compared with unity for any pair of modes, in order that the N modes may coexist. (The condition is $\beta \ll 1$ for $N=2$, but it may be more drastic for larger N). The expression of the Landau coefficient and its law of variation as a function of the angle θ is determined from the equations of the system.

IIa- Polarization instability case

The Landau coefficient¹⁰ obeys the quite simple law,

$$\beta(\theta) = \left(1 + \frac{1}{\chi}\right) - \left(1 - \frac{1}{\chi}\right) \cos[2K_c^2 \cos(\theta)],$$

where χ is the nonlinearity parameter. It displays deep oscillations with minima equal to $2/\chi$, located at

$$\theta = \cos^{-1}(k\pi / K_c^2), \text{ where } k = 0, 1, \dots \quad (4)$$

Let us consider the case of an excitation on the defocusing side of the rubidium transition so that the linear stability analysis provides

$$K_0^2 = \frac{3\pi}{2}. \quad (5)$$

For this value of the critical wavenumber, the minima of $\beta_{1\ell}$, where the mode "1" is at $\theta=0$, are located at $\theta_{12} = \cos^{-1}(\frac{2}{3}) \cong \frac{\pi}{4}$, $\theta_{13} = \frac{\pi}{2}$, $\theta_{14} = \cos^{-1}(\frac{4}{3}) \cong \frac{3\pi}{4}$, as shown in Fig. 2a.

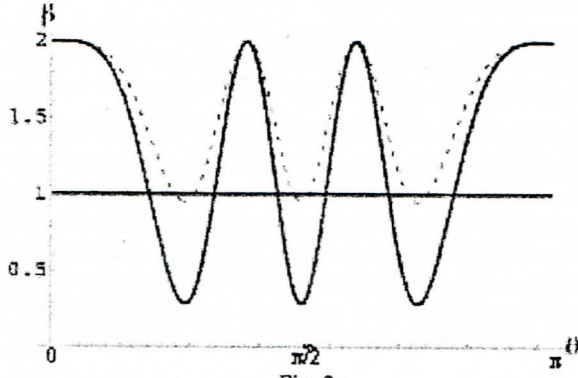


Fig. 2a

For $\chi = 7$ in full line and $\chi = 2.1$ in dashed line

Therefore, with such a repartition on the half circle, the other Landau coefficients β_{23} , β_{24} , and β_{34} , are also very close to zero. This leads to the prediction that eight Fourier modes coexist on the full circle, and consequently to the formation of an eightfold orientational order quasipattern^{10a}. Indeed, the calculation of the free energy^{10b} has confirmed that this structure is the most stable in the limit for $\chi \geq 2.17$.

The situation is different for larger critical wavenumbers K_n , see Eq. (1): It is easy to deduce from the variation law of the Landau coefficient with respect to θ in Eq. (4) that the number of zeros increases and that they are not regularly distributed on the circle. This irregular distribution of the modes on the circle implies that the vertex angle between any two modes is not necessary close to an angle satisfying the relation (4). Some $\beta_{p\ell}$, ($p, \ell \neq 1$), can be even greater than unity because of the steep variation of the Landau coefficient between two extrema. For this reason, the polarization instability only generates the eightfold orientational order quasipattern. Far enough above threshold, this structure bifurcates to a multicritical pattern^{10b}, basically composed of rhombuses with side length equal to $\frac{2\pi}{K_0}$.

IIb- Dopo

In this case, the successive critical wavenumbers are $K_n = \sqrt{\delta_1 + n\pi}$, where δ_1 is the cavity mistuning of the signal. The analytical expression⁴ of $\beta(\theta)$ is quite complicated and is not given here. Its angular variation law is reported in Fig. 2b in the case of two different critical wavenumbers K_1 and K_2 , where quasipatterns may be expected. The Landau coefficient associated with K_1 displays a plateau close to zero for a large domain of θ , as shown by the full line of Fig. 2b, so that several regularly distributed modes may coexist; for $K_c = K_2$, in dashed line, $\beta(\theta)$ exhibits sharp peaks at θ close to $\pi/2$. (Here the mistuning is equal to -0.1 , but the same qualitative behaviour is displayed if the mistuning has the opposite sign). As K_c increases further, the number of maxima larger than unity also increases, so that the formation of quasipatterns becomes unlikely.

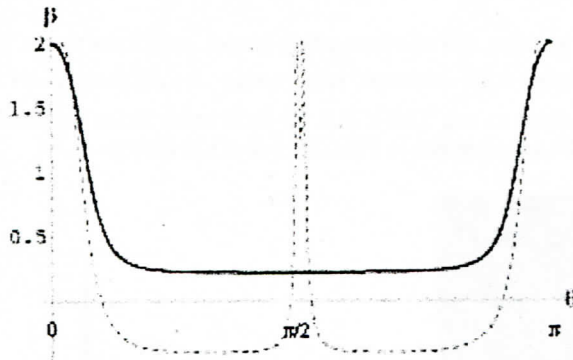


Fig. 2b

Numerical simulations are shown in Figs. 3a-3f in the case where the threshold intensity degeneracy is removed, due to losses during the free-space propagation of the light beams. Therefore, for small enough intensity, only the lowest critical wavenumber is involved.

The far-field intensity in Fig. 3b displays eight peaks regularly distributed on a circle of radius K_1 that agrees with the prediction in Fig. 2b. The near-field intensity is composed of octagonal cells, as seen in Fig. 3a and is clearly not invariant by translation in any direction of the transverse plane. The quasiperiodic character of the pattern is displayed in Fig. 3c where the variation of the intensity along a straight line of the plane (x,y) is drawn.

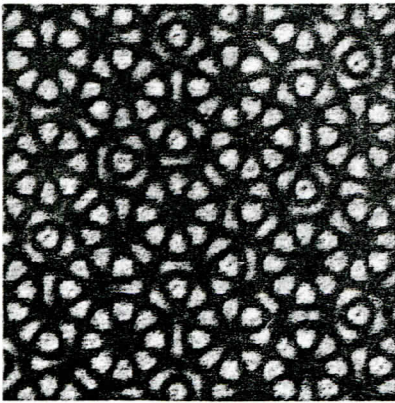


Fig. 3a



Fig. 3b

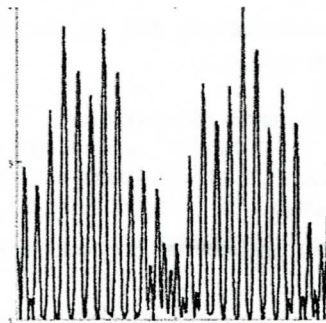


Fig. 3c

This monoconical quasistructure becomes unstable when the input intensity increases to twice the threshold intensity. The secondary bifurcation displays a biconical pattern involving both K_1 and K_2 . Next, the biconical structure bifurcates to a monocritical structure with $K_c = K_2$, for an input intensity about four times the threshold intensity, as shown in Figs. 3d-f. This structure remains stable for an input intensity about sixteen times the threshold one. It is composed in the far-field of ten peaks irregularly distributed on the circle, as shown in Fig. 3e. It appears so far above threshold that the behaviour of Landau coefficient, (the dashed line in Fig. 2b), gives only a qualitative idea of the far-field geometry. The variation of the near-field intensity in Fig. 3d along any straight line of the transverse plane looks chaotic, because the critical wavenumber and two chords of different lengths are involved, (see Fig. 3f). Let us also point out the presence of very small peaks on the inner circle of radius K_1 , which are not

visible in Fig. 3d. While passive, the corresponding modes contribute to the formation of the structure via the cubic interaction between two modes $\bar{K}_{2,\ell}$ and $\bar{K}_{2,p}$ on the circle K_2 , making the vertex angle close to $\cos^{-1}(3/4)$. If a far-field mask hides the small wavenumbers centered about K_1 , then the quasipattern in Figs. 3d-f does not emerge.

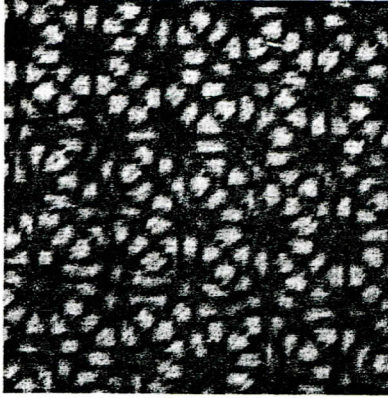


Fig. 3d



Fig. 3e

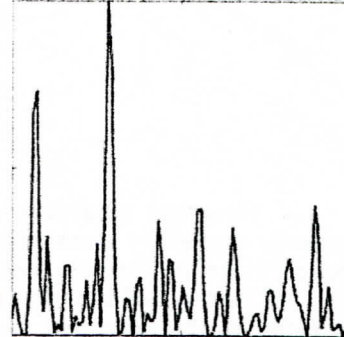


Fig. 3f

Actually, while monocritical, these quasistruktures are reinforced due to multicriticality. For instance, the two sets of passive modes with wavenumbers $\sqrt{2}K_1$ and $2K_1$ generated via the nonlinearities from $\{\bar{K}_1\}$ are closely in resonance with the critical wavenumbers K_2 and K_4 , respectively, when choosing a cavity mistuning of the signal δ_1 , small enough.

III-Bicritical bifurcations

H. Müller²³ considered a mechanism involving a coupling between two sets of active modes regularly distributed on two concentric circles of radii equal respectively to the critical wavenumbers K and q . First, he treated the case of eight modes on each circle: Then, the triadic interaction between modes gives rise to $\bar{K}_1 + \bar{K}_2 = \bar{q}_1$ with $(\bar{K}_1, \bar{K}_2) = \frac{\pi}{4}$ and

$\frac{q}{K} = \sqrt{2 + \sqrt{2}}$, such that the outer set of modes is twisted by the angle $\frac{\pi}{8}$ with respect to the

inner set. For twelve modes, the magic ratio can be $\sqrt{2 + \sqrt{3}}$ and the outer set of modes is twisted by the angle $\frac{\pi}{6}$. The magic ratio can be also $\sqrt{2}$ that only couples orthogonal modes.

In the model chosen by Müller for the envelope equations, the quasipatterns are preferred in presence of a coupling between the bicritical sets of modes, while squares (hexagons) prevail when the coupling vanishes.

Here the mechanisms for the formation of two different optical bicritical structures are analyzed and compared with those proposed by Müller.

IIIa)-Bisquares

We analyze the patterns observed in the simulations of a passive ring cavity with a dispersive quasi-Kerr medium, illuminated by a cw red-shifted pump beam¹¹. On the defocusing side of the atomic resonance, the successive critical wavenumbers are close to

$K, \sqrt{2}K, \sqrt{3}K, 2K$. With a low-pass filter transparent to the first three cones, biconical patterns occur, built up with the K and $\sqrt{2}K$ wavenumbers.

Near the onset of instability, a stable bisquare pattern spontaneously emerges from noise, or grows from a strong initial hexagonal modulation, displaying two sets of active orthogonal modes $\{\vec{K}, \sqrt{2}\vec{K}\}$ that drastically change the hexagonal order corresponding to a monocritical set of active modes. Indeed, the near-field pattern (Fig. 4a) looks like two sets of intricate squares.

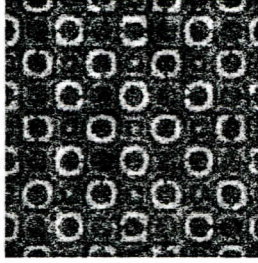


Fig. 4a

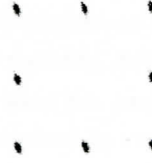


Fig. 4b

The basic set presents a large modulation $\frac{2\pi}{K}$, with bright peaks separated by a secondary square structure of modulation $\frac{\sqrt{2}\pi}{K}$. The far-field consists of two sets of four spots distributed in quincunx, see Fig. 4b.

The weakly nonlinear analysis in the vicinity of the instability boundary was developed in details for the case of the bisquare pattern in Ref. [11]. The stationary patterns display amplitudes $\{A_i\}$ on the inner ring that are twice larger than the amplitudes $\{B_i\}$ on the outer ring, leading to the first order solution $Q + Q'$, with

$$Q = A_1 e^{iKx} + A_2 e^{iKy} + c.c., \quad \text{and} \quad Q' = B_1 e^{iK(x+y)} + B_2 e^{iK(x-y)} + c.c. \quad (6)$$

The multiple scale analysis associated to the bicritical solution (6) leads to the following set of coupled equations for the amplitudes of the Fourier modes,

$$\begin{aligned} \partial_t A_1 &= \mu A_1 + \gamma \frac{A_2^* B_1 + A_2 B_2^*}{2} + A_1 (\delta |A_1|^2 + \beta |A_2|^2) + \sigma A_1^* B_1 B_2 + \chi A_1 (|B_1|^2 + |B_2|^2) \\ \partial_t A_2 &= \mu A_2 + \gamma \frac{A_1^* B_1 + A_1 B_2^*}{2} + A_2 (\delta |A_2|^2 + \beta |A_1|^2) + \sigma A_2^* B_1 B_2 + \chi A_2 (|B_1|^2 + |B_2|^2) \quad (7) \\ \zeta \partial_t B_1 &= \mu' B_1 + \gamma' A_1 A_2 + B_1 (\delta' |B_1|^2 + \beta' |B_2|^2) + \sigma' (A_2^2 B_2 + A_1^2 B_2^*) + \chi B_1 (|A_1|^2 + |A_2|^2) \\ \zeta \partial_t B_2 &= \mu' B_2 + \gamma' A_1 A_2^* + B_2 (\delta' |B_2|^2 + \beta' |B_1|^2) + \sigma' (A_2^{*2} B_1 + A_1^2 B_1^*) + \chi B_2 (|A_1|^2 + |A_2|^2) \end{aligned}$$

In these equations, the quadratic coupling terms proportional to γ and γ' describe the resonant triadic interaction between the two active sets $\{\bar{K}, \sqrt{2}\bar{K}\}$, and the negative values of δ, δ', σ and σ' ensure the stability for positive μ and μ' . The comparison of the stationary solutions of Eqs. (7) with the numerical amplitudes is quite satisfying¹¹. Furthermore the study of the behaviour of the cubic coupling coefficient β between modes $\{\bar{K}\}$ shows that the angle $\frac{\pi}{2}$ is preferred in the case of a bicritical instability, while it shifts to $\frac{\pi}{3}$ for a monocritical instability. This last result confirms the existence of a square structure for the biconical case and of a hexagonal structure in the monoconical situation. Furthermore, the monoconical process is unable to foresee the biconical structure because the corresponding $\beta(\frac{\pi}{2})$ has a large negative value that would lead to unstable squares.

In conclusion, although the $\{\bar{K}, \sqrt{2}\bar{K}\}$ triadic coupling is involved in the formation of the bisquare structure, the basic symmetry of the monoconical pattern is lost. That example illustrates the variety of biconical patterns that may result from the $\{\bar{K}, \sqrt{2}\bar{K}\}$ coupling and shows that the symmetry of the monocritical structure is not necessarily preserved.

IIIb) Twelvefold orientational order quasipattern.

In the case of the single-feedback mirror with a rubidium cell, driven by a red-shifted pump beam with respect to the atomic resonance line, the magic ratio for the occurrence of a twelvefold quasipattern is almost satisfied between the two critical wavenumbers $\sqrt{\frac{11\pi}{2}}$ and $\sqrt{\frac{3\pi}{2}}$, corresponding respectively to K_4 and to K_0 as given in Eqs. (4) and (5). Therefore, the basic mechanism of a triadic coupling between the two sets of modes associated with the above wavenumbers should work when the device presents a Kerr-like nonlinearity. This happens when the pump beam is circularly polarized, for instance clockwise. Then, the nonlinear part of the refractive index of the light Q , which is proportional to the population difference between the two lower states of the atomic transition $5S_{1/2} \rightarrow 5P_{1/2}$, obeys the equation

$$\partial_t Q = -(1 + I_+)Q - I_+, \quad I_+ = I_0 \left(1 + \left| \text{Re}^{iL\nabla^2} e^{iQ} \right|^2 \right), \quad (8)$$

where I_+ is the sum of the input intensity I_0 and of the intensity of the light beam reflected by the plane mirror located at the distance $L/2$ from the cell exit, with reflectivity factor R . (Absorption effects are supposed to be negligible). The equation (8) differs from the equation for a linearly polarized pump beam, mainly by the source term, which, above threshold, displays an electric field component with polarization orthogonal to the pump one. In the case described by Eq. (8), the nonlinear refractive index possesses a homogeneous stationary component proportional to the input intensity, like in Kerr media. For a monocritical bifurcation, the hexagonal symmetry is well-known to appear, so that it is reasonable to expect a twelvefold quasipattern when a bicritical bifurcation can occur with the condition $\frac{q}{K} \approx \sqrt{2 + \sqrt{3}}$. Actually, the numerical simulations display the quasipattern composed of basic cells made of twelve peaks, as shown in Fig. 5a. The far-field displays twelve intense spots on a circle of radius K in Fig. 5b.

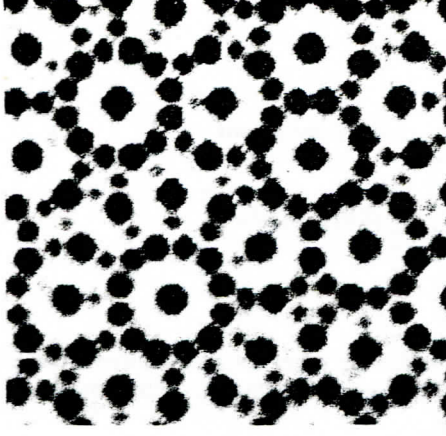


Fig. 5a

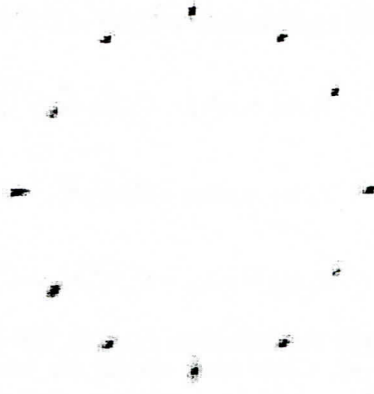


Fig. 5b

The twelve peaks corresponding to the largest wavenumber q are so weak that they are not visible on the figure. This feature indicates that the modes associated with the larger wavenumber q can be treated as passive modes²⁴. This assumption simplifies considerably the multiple scale analysis, leading to the expansion

$$Q = \sum_{j=1}^3 A_{1j} e^{i\bar{K}_{1j}\bar{r}} + A_{2j} e^{i\bar{K}_{2j}\bar{r}} + c.c. , \quad (9)$$

where Q is the sum of two sets of modes with amplitudes $\{A_{1j}, A_{1j}^*\}$ and $\{A_{2j}, A_{2j}^*\}$ forming two hexagons tilted by the angle $\pi/6$ with

$$\{ \bar{K}_{11} = (K_c, 0), \bar{K}_{12} = (-\frac{1}{2}K_c, \frac{\sqrt{3}}{2}K_c), \bar{K}_{13} = (-\frac{1}{2}K_c, -\frac{\sqrt{3}}{2}K_c) \}, \quad (10a)$$

and

$$\{ \bar{K}_{21} = (0, K_c), \bar{K}_{22} = (-\frac{\sqrt{3}}{2}K_c, -\frac{1}{2}K_c), \bar{K}_{23} = (\frac{\sqrt{3}}{2}K_c, -\frac{1}{2}K_c) \}. \quad (10b)$$

Losses are introduced during the free-space propagation that amount to replacing the diffraction operator $e^{i\nabla^2 L/2k}$ by $e^{i\nabla^2 L/2k(1-i\sigma)}$ with real σ , so that the threshold intensity increases exponentially with K .

The multiple scale analysis of Eqs. (8) gives rise to

$$\begin{aligned}
 \partial_t A_{11} &= \mu A_{11} - C_2 A_{12}^* A_{13}^* - C_3 A_{11} \sum_{m=1}^2 \sum_{n=1}^3 \beta(\theta_{11,mn}) |A_{mn}|^2 \\
 \partial_t A_{12} &= \mu A_{12} - C_2 A_{13}^* A_{11}^* - C_3 A_{12} \sum_{m=1}^2 \sum_{n=1}^3 \beta(\theta_{12,mn}) |A_{mn}|^2 \\
 \partial_t A_{13} &= \mu A_{13} - C_2 A_{11}^* A_{12}^* - C_3 A_{13} \sum_{m=1}^2 \sum_{n=1}^3 \beta(\theta_{13,mn}) |A_{mn}|^2
 \end{aligned} \tag{11}$$

with the definitions (9)-(10). The equations for the other set are deduced from Eqs. (11) by $1 \rightarrow 2$. Cubic terms display the interaction between two adjacent active modes, for instance \bar{K}_{11} and \bar{K}_{21} that make the vertex angle $\pi/6$.

The comparison between the analytical prediction for the stationary amplitudes and the numerical simulations is displayed in Fig. 5c. Their qualitative good agreement confirms the validity of the single active mode approximation (9).

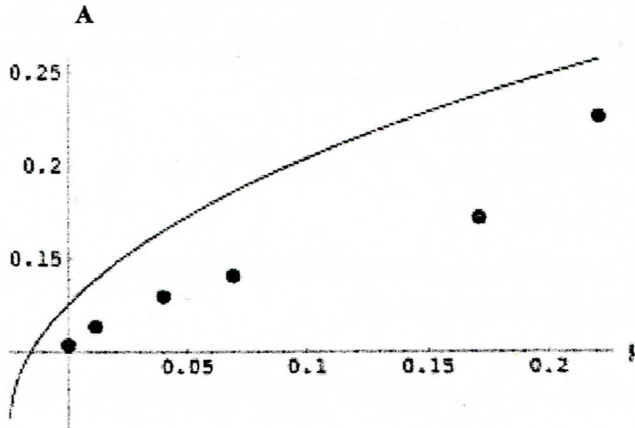


Fig. 5c

The formation of the twelvefold quasipattern was also analytically studied in Ref. [13]. The authors use a modal decomposition based on a von Neumann-Karmann expansion and derive some amplitude equations for two sets of active modes using a perturbation method. This method does not take any solvability condition into account. Therefore, there is no evidence that the modal decomposition involving two sets of active modes gives rise to better predictions than our amplitude equations (12) for a single set of active modes.

The system under study is variational, so that it is easy to determine the most stable structure, either the hexagonal pattern or the twelvefold quasipattern as the loss parameter σ is varied. The quasipattern is expected to occur for small losses, when the threshold intensity associated with the critical wavenumber q is not too high. Analytical predictions and numerical results were shown to be in good agreement.

IV-Conclusion

In a general manner, multicriticality can induce a very rich variety of structures. This has been successfully treated, using the multiple scale analysis expansion either for a single set or for two sets of active modes. In the case of a monocritical instability, the number of Fourier modes that may coexist crucially depends on the shape of the Landau coefficient. In the DOPO, the shape of the Landau coefficient is very sensitive to the pump and signal mistunings²⁵ and it happens that for some values of this parameter, $\beta(\theta)$ presents a large plateau on which more than eight or ten modes would be allowed to coexist on the full circle: For instance, a ten-fold orientational order quasipattern has been obtained for $\delta_1 = -0.5$ and δ_0 close to $2\delta_1$; a twelve- mode structure has been also observed that displays a periodic pattern, in which flowers of twelve petals form a square lattice, as a result of a locking effect. However, we have not yet found a Landau coefficient satisfying the condition for turbulent quasipatterns, as discussed by Newell and Pomeau²⁶.

Finally, let us emphasize that the many-mode patterns arise for large critical wavenumbers, approximately two or three times larger than the smallest one, leading to rolls squares or hexagons. It follows that the condition of large aspect ratio is more easily satisfied for the observation of quasipatterns.

Acknowledgements

The numerical simulations have been realized with the CRAY C90 of the IDRIS CNRS computer center, and the results have been treated at the CRI of the Université Paris-Sud. The authors greatly acknowledge the IDRIS center and the CRI for their services.

References

- 1- Special Issue on Transverse Effects in Nonlinear Optical Systems, ed. Abraham N.L. and Firth W. J., *JOSA*, B6-7 (1990); Transverse Patterns in Nonlinear Optics, ed. Rosanov N.N, Mak A.A., Grasiuk A.Z., SPIE, 1991; Special Issue on Nonlinear Optics Structures, Patterns, Chaos, ed. Lugiato L.A. and El Naschie M.S., in *Chaos, Solitons & Fractals*, 4(1994).
- 2- Patrascu A.S., Nath C., Le Berre M., Ressayre E. and Tallet A., *Optics Commun*, 91(1992)433; D'Alessandro G. and Firth W.J., *Phys Rev A*, 4(1992)537; Le Berre M, Patrascu S., Ressayre E., Tallet A. and Zheleznykh N.I., *Chaos, Solitons & Fractals*, 4(1994)1389; Geddes J.B., Lega J., Moloney J.V., Indik R.A., Wright E.M and Firth W.J., *Chaos Solitons & Fractals*, 4(1994)1261; Vorontsov M.A., Iroshnikov N.G., and Abernathy R.L, *Chaos, Solitons & Fractals*, 4(1994)1701.
- 3- Lugiato L.A. and Lefever R., *Phys Rev Lett*, 58(1987)2209.
- 4- Le Berre M., Leduc D., Patrascu S., Ressayre E. and Tallet A. , *Chaos, Solitons & Fractals*, to appear
- 5- Thuring B., Neubecker R., Tschudi T., *Chaos, Solitons & Fractals*, 4(1994)1307.
- 6- Staliunas K., Slekyas G., Weiss C.O., *Phys Rev Lett*, 79(1997)2658.
- 7- Mamaiev A.V., and Saffman M., *Optics Commun*, 128(1996)281.
- 8- Pampaloni E., Ramazza P.L, Residori S., Arecchi F.T., *Phys Rev Lett*, 74(1995)258.
- 9- Golovin A.A, Nepomnyashchy A.A., Pismen L.M., *Physica D*, 81(1995)117.
- 10- a) Leduc D., Le Berre M., Ressayre E. and Tallet A., *Phys Rev A*, 53(1996)1072, b) *Opt Commun*, 130(1996)181 and c) *Phys Rev A*, 55(1997)2321.
- 11- Le Berre M., Leduc D., Ressayre E. and Tallet A., *Phys Rev A*, 54(1996)3428.
- 12- Degtiarev E.V. and Vorontsov M.A, *J Mod Opt*, 43(1996)93.
- 13- Vorontsov M.A. and Karpov A.Yu., *JOSA B*, 14(1997)34.
- 14- Rubinstein B.Y and Pismen L.M., to appear in *Phys Rev A* and to appear in *Chaos, Solitons & Fractals*, (1998).

- 15-a) Herrero R., Buthe E., Logvin Yu. A., Aumann A., Ackemann T., Lange W., Patterns in Nonlinear Optics (PINOS) Abstracts, 1998; b) Herrero R., E. Grosse-Westhoff E., Logvin Yu. A., Aumann A., Ackemann T., Lange, to be submitted. W
- 16-Levine D. and Steinhardt P.J., *Phys Rev Lett*, 53(1984)2477.
- 17-Shechtman D. et al, *Phys Rev Lett*, 53(1984)1951.
- 18-The Physics of Quasicrystals, edited by Steinhardt P.J and Ostlund S. (World Scientific, Singapore), 1987; Introduction to Quasicrystals, edited by M.V. Jaric (Academic Press, Boston), 1988; Introduction to the Mathematics of Quasicrystals, edited by M.V. Jaric (Academic Press, Boston), 1989; Lectures on Quasicrystals, edited by Hippert F. and Gratias D., (Les Editions de Physique, Paris), 1994.
- 19- Guidoni L., Triche C., Verkek P., and Grynberg G., *Phys Rev Lett*, 79(1997)3363.
- 20- Edwards Stuart W. et Fauve Stéphane, *C.R.Acad Paris*, 315(1992)417; and *Phys Rev E*, 47(1993)R788.
- 21- Christiansen Bo, Preben Alstrom, and Mogens T. Levinsen, *Phys Rev Lett*, 68(1992)2157.
- 22- Binks Doug and van de Water Willen, *Phys Rev E*, 78(1997)4043.
- 23- Müller Hanns Walter, *Phys Rev E*, 49 (1994)1273.
- 24- Leduc D "Structures Transverses Quasiperiodiques en Optique et Multicriticalite" PhD Thesis, (Université de ParisVI, 1998).
- 25- Le Berre M. et al, in preparation.
- 26-Newell A.C. and Pomeau Y., *Phys .A: Math Gen*, 26(1993)L429.

OPTIČKE KVAZIMUSTRE

M. Leber, D. Ledik, E. Resair, A. Tale

Kvaziperiodične strukture potiču od multikritičnosti. Mehanizmi nastanka ovakvih struktura analizirani su za optičke uređaje koji pokazuju različite oblike nelinearnosti. Numeričke mustre potvrđuju predviđanja analize višestrukog skaliranja.